https://chemclassjournal.com/
ChemClass Journal Vol. 9 Issue 3 (2025); 334 - 354
e-ISSN:3092-8214 p-ISSN:3092-8206
doi.org/10.33003/chemclass-2025-0903/26

Evaluation of *Hunteria umbellata* Extracts as Green Corrosion Inhibitors for Mild Steel in Corrosive Environments

Adio, O.[1*], Ogunleye, O.O[2], Arinkoola, A. O[3]

[1]*Department of Chemical Engineering Technology, Kwara State Polytechnic, Ilorin, Kwara State, Nigeria*
[2]*Department of Chemical Engineering, Ladoke Akintola University of Technology, Ogbomoso, Nigeria*
[3]*Department of Chemical Engineering, Ladoke Akintola University of Technology, Ogbomoso, Nigeria*

***Corresponding author:** Email: **adio.oseni @ gmail.com**; Phone no/WhatsApp: **08134224023**

Abstract

This study investigates the corrosion inhibition potential of *Hunteria umbellata* extracts on mild steel in acid, salt and alkali corrosive environments. *Hunteria umbellata* methanolic crude extracts (HUCE) and their phytomolecules such as Alkaloid (HUAE), Flavonoid (HUFE), Saponin (HUSE), and Tannins (HUTE) were characterized using Gas Chromatograph- Mass Spectroscopy (GC-MS) and Fourier Transform Infra-Red (FTIR) spectroscopy. Corrosion inhibition study was carried out using gravimetric methods; depth of attack, electrochemical techniques. The crude extract exhibited the highest inhibition efficiency of 95.17% in 1M HCl. However, the increasing order of performance of the phytomolcules (89 – 90%) in all these media is alkaloid > saponin > tannin > flavonoid. Adsorption of inhibitors followed Langmuir isotherm and pseudo-second-order kinetics. Thermodynamic studies indicated spontaneous, endothermic and physical adsorption process. The crude extract effectively reduced the weight loss over time when applied as a coating. The results demonstrate the potential of *H. umbellata* as an environmentally benign alternative to synthetic inhibitors.

Keywords: Corrosion inhibitors, *Hunteria umbellata*, Isotherm, Mildsteel, Phytomolecules

1.0 Introduction

Mild steel (MS) is extensively utilized in construction, oil and gas, chemical processing, and water transportation owing to its mechanical strength, malleability, weld ability, and cost-effectiveness [1] However, its susceptibility to corrosion in acids, salts, and alkali environments affect its durability and escalates maintenance costs. Metallic corrosion poses a significant economic and safety challenge [2]. Global corrosion-related losses are anticipated to surpass USD 2.5 trillion per year, representing roughly 3.4% of the world's GDP [3]. Conventional corrosion mitigation methods encompass cathodic protection, surface coatings, material selection, and corrosion inhibitors [4].

© CSN Zaria Chapter

Notwithstanding, the use of corrosion inhibitors are both economical and effective, especially for internal surfaces. Synthetic inhibitors are toxic, not biodegradable, and unfriendly to environment, therefore necessitating a transition to eco-friendly inhibitors. Plant-derived inhibitors have garnered interest owing to their biodegradability, availability, and environmental sustainability [5]. Plant extracts are rich in phytochemicals such as alkaloids, tannins, flavonoids, and saponins, which possess heteroatoms (N, O, S) and pi-electrons that promote adsorption on metallic surfaces [6]. Much comprehensive research has been documented on the efficacy of plant extracts as corrosion inhibitors [7].

The commercial utilization of green inhibitors is however limited owing to lack of sufficient design and detailed analysis of the inhibitor. Hence, this study investigates the corrosion inhibition potentials and the synergistic effects of some active compounds isolated from *Hunteria umbellata* seed towards mild steel in acid, alkali and salt environments. The pictorial view of the *Hunteria umbellata* seed plant is presented as shown in Plate 1



Plate 1: ***Hunteria umbellata* seed**

2.0 Methodology

2.1 Materials and Equipment

Mild steel coupons, *Hunteria umbellata* seed, distilled water and analytical reagents (hydrochloric acid, sodium hydroxide, sodium chloride, methanol, ethanol, ethyl acetate and acetone) were procured from nearby markets in Ilorin, Nigeria. The equipment used includes soxhlet extractor, rotary evaporator, oven, thermostatic water bath, weighing balance and PCE-RT 11 surface tester. For qualitative analysis, Gas Chromatography/Mass Spectrophotometer (GC-MS), Fourier Transform Infra-Red (FTIR) Spectrophotometer and Scanning Electron Microscope (SEM). Other apparatus and consumables include emery paper, ceramic mortar and pestle, glass separating funnels, measuring cylinder, conical flask, filter paper, and desiccators.

2.2 Extraction, Isolation and Characterization of Extracts

The dried samples were pulverised and screened to approximately 2µm to increase their surface areas, and kept in an air-tight cellophane bag. The extraction of the phyto constituents from powder material was done using soxhlet extractor with methanol as the solvent. The extract was concentrated using rotary evaporator and stored at 4^{o}C in an air- tight sterile containers [8]. Extraction of alkaloids (HUAE) saponins (HUSE), flavonoids (HUFE) and tannins (HUTE) was carried out according to [9]. The chemical

composition of the extract was determined using GC-MS analysis. FTIR spectroscopy was employed to ascertain functional groups. Scanning Electron Microscopy (SEM) was employed to analyse the surface morphology of steel samples with or without inhibitors.

2.3 Corrosion study

Mild steel coupons (3 cm×2 cm× 0.3 cm) of 0.18% carbon, 0.68% manganese, 0.03% sulfur, 0.04% phosphorus and 99.07% iron were used after cleaned in acetone and dried. The three media1M HCl, NaOH and NaCl were prepared using standard method. Solutions of varying concentrations (0 – 1.2 g/L) of the crude extracts and isolated alkaloids, saponins, flavonoids, and tannins were prepared and stored in desiccators [10].

2.3.1 Weight loss method

Weight loss of Mild steel coupons submerged in 100ml corrosion solution in the absence and presence of different concentrations of the *Hunteria umbellata* crude extract (0 - 1.2 g/L) was determined at 30^{O}C after 24, 48, 72, 96, 144 and 168 h using full factorial design. Each coupon was weighed before immersion (m_1) and retrieved from the test solution at various time then reweighed (m_2). The corrosion rate was calculated from Equations (1–4).

$$W = m_1 - m_2 \quad (1)$$

$$CR = \frac{W}{A \times T} \quad (2)$$

$$IE = \left[\frac{CR_0 - CR_1}{CR_0}\right[\times 100\ \% \quad (3)$$

$$\theta = \frac{IE}{100} \quad (4)$$

Where, CR is the corrosion rate of the coupon of surface area (A, cm^2) over time t (h). W is the weight loss. θ is the degree of inhibitor surface coverage and IE the inhibition efficiency.

2.3.2 Depth of attach profile method

The corrosion depth of attack was measured using a surface roughness tester (PCE-RT11). The maximum height of irregularities (Rz) was measured over a sampling length of 2.5 mm. The measurement was taken before and after corrosion. The corrosion rate of MS in terms of R_Z was calculated using Equations (5-7)[10].

$$\Delta R_Z = R_{Zf} - R_{Zi} \quad (5)$$

$$CR_{R_Z} = \frac{\Delta R_Z}{l \times t} \quad (6)$$

$$IE_Z = \left(\frac{r^O_{R_Z} - r^I_{R_Z}}{r^O_{R_Z}}\right) \times 100\ \% \quad 7)$$

2.4 Adsorption isotherm determination

The degree of surface coverage, θ, for varying inhibitor concentration at room temperature was used to elucidate the adsorption isotherm to establish the adsorption processes involved. The following isotherms were evaluated graphically.

2.4.1 Langmuir isotherm

Langmuir adsorption isotherm is given by Equations (8) and (9):

$$\frac{C}{\theta} = \frac{1}{K_{Ads}} + C \quad (8)$$

$$K_{Ads} = \frac{1}{55.5} exp\left(-\frac{\Delta G^0_{Ads}}{RT}\right) \quad (9)$$

Where C is the concentration of the inhibitor in the bulk solution (g/L), θ is the surface coverage of the inhibitor, and K_{Ads} is the adsorption

equilibrium constant (L/g). The 55.5 represents the concentration of water in solution expressed in g/L, R is the gas constant, and T absolute temperature [10].

2.4.2 Freundlich isotherm

The linearised form of the Freundlich adsorption isotherm is given by Equation (10), and a plot of log θ against log C yields the parameters n and K_{Ads}

$$\log \theta = \log K_{Ads} + 1/n \log C \quad (10)$$

2.4.3. Temkin isotherm

The degree of surface coverage (θ) is related to inhibitor concentration (C) according to Equation (11).

$$e^{-2a\theta} = KC \quad (11)$$

Where K is the adsorption equilibrium constant and a is the interaction parameter. Rearranging and taking the logarithm of both sides of Equation (11) gives Equation (12), and θ will be plotted against log C

$$\theta = \frac{-2.393 \log K}{2a} + \frac{-2.303 \log C}{2a}. \quad (12)$$

2.5 Corrosion inhibition kinetics

To determine the optimum concentration of the inhibitors, it is necessary to explore the dynamics of their inhibition. The two kinetic models considered in this study, are pseudo-first and second order kinetic models, are presented by Equations 13 and 14, respectively.

$$\frac{d\theta}{dt} = k_1(\theta_e - \theta_t). \quad (13)$$

$$\frac{d\theta}{dt} = k_2(\theta_e - \theta_t)^2 \quad (14)$$

K_1 and K_2 (min^{-1}) are the rate constants were obtained graphically following integration within the necessary boundary limits. θe and θt represent the degree of surface coverage at equilibrium and at a given time t.

2.6 Thermodynamic study

To determine the energy required, the heat involved and the mechanism of corrosion in the presence or absence of an inhibitor, the following thermodynamic properties were determined graphically: the activation energy (Ea), enthalpy (ΔHa), and entropy (ΔSa) using the Arrhenius Eq. (15), the transition state Equation (16), and the Free Gibb energy of the adsorption (G_{ads}) equation (17).

$$C_R = A \exp\left(-\frac{E_a}{RT}\right) \quad (15)$$

$$C_R = \frac{RT}{Nh} \exp\left(\frac{\Delta S_a}{R}\right) \exp\left(-\frac{\Delta H_a}{RT}\right) \quad (16)$$

$$G_{ads} = 2.303\ RT \log (55.5K) \quad (17)$$

T represents the absolute temperature. A is the pre-exponential factor. N is Avogadro's number (6.02×10^{23} mol^{-1}), h is Planck's constant (6.63×10^{-34} J s^{-1}), K is the equilibrium constant, and the constant denoted by 55.5 denotes the molar heat of adsorption of water.

2.7 Application of HUCE in Coating

The incorporation of the methanolic extracts into alkyd resin paint was done according to the formulations in Table 1. The coating mixture was stirred for 1 hour for each concentration. A brush was used to apply the coating on the already prepared metal surface because it provides very high shearing forces between the liquid paint and

the substrate. Equation (18) was used to determine the concentration of the plant extract.

$$concentration(^{v}/_{v})\% = \frac{solubleextract(ml)}{solventpaint(ml)} \times 100\ \% \quad (18)$$

The coated plate of the mild steel was tested for its anti-corrosive performance using a weight loss experiment in the corrosive environments. The weight reduction was observed over a 5-week immersion period with data collection done every week. [23] .

Table 1 Coating formulation for the concentration of extracts

Plant extract (ml)	Alkyd paint (ml)	Concentration of plant (v/v %)
Control (0.0)	66	0.00
0.2	66	0.30
0.3	66	0.45
0.4	66	0.60

3.0 Results and Discussion

3.1 Phytochemical screening

The qualitative analysis of the phytochemicals present in the crude extracts of *Hunteria umbellata* plant was carried out. The phytochemical screening of non-volatile crude extracts of *Hunteria umbellate* seed revealed the presence of steroid, triterpenes, alkaloid, tannins, flavonoid, lactone, glycosides, diterpenes and saponin as presented in Table 2. The isolated organic compounds from the crude extract yielded 3.31% alkaloids, 0.92% flavonoids, 2.98% tannins, and 1.06% saponins. These compounds possess characteristic hetero atoms in their molecular structure, which serve as a good site for adsorption onto the metal surfaces [8].

Table 2: Phytochemical screening for the Methanolic extract of *Hunteria umbellata* seed

S/N	Organic extracts	Result
1.	Steriod	+
2.	Triterpenes	++
3.	Alkaloid	++
4.	Tannins	++
5.	Flavonoid	+
6.	Lactone	+
7.	Diterpenes	+
8.	Glycoside	+
9	Saponins	+

Key: ++ *strong present* + *present* - *absence*

3.2 GC-MS Analysis of the chemical constituents of HU seed extracts

The GC-MS chromatographs depicted in Figure 1 shows the chemical composition of the *Hunteria umbellata* crude extract (HUCE).Table

3 displays the chemical constituents and percentage composition of the non-volatile crude extract of HU seed. The total yield of the methanolic crude extract was 9.87 % (v/w). Eighteen compounds at different peaks and retention time were identified. The two dominant compounds are pyridine, 3-ethyl at highest peak value of 44.99% and retention time of 3.138 min and 9-Octadecenoic acid, at peak value of 21.21% and retention time of 15.252 min. The presence of amide, carboxylic acid, ester, hydroxyl, and phenyl suggest adsorption of these compounds onto metal surface [6][11].

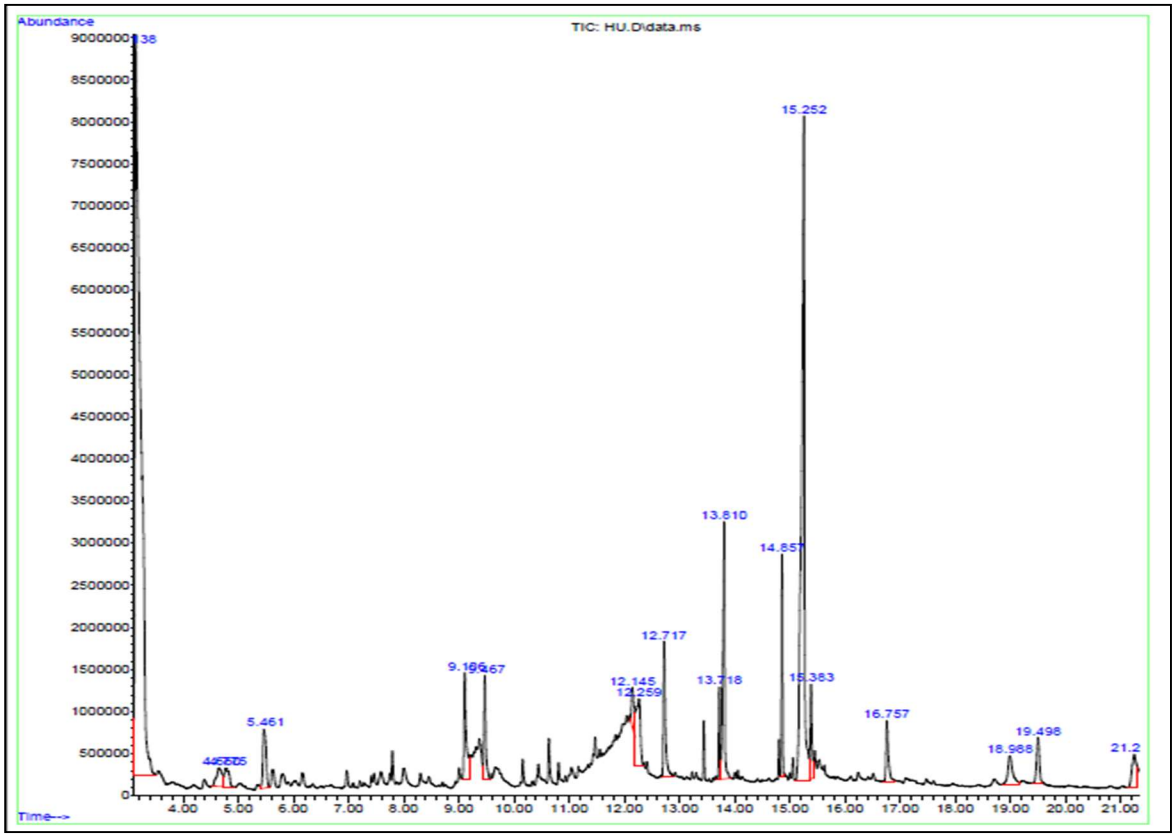


Figure 1: *Hunteria umbellata* methanolic extract (HUCE) GC-MS chromatograph

Table 3 Chemical constituents and their percentage composition in HUCE seed extract

S/N	Compound	%Similarity Index	Retention Time (min)	% Composition
1	Pyridine, 3-ethyl-	97	3.138	44.99
2	Pyrazine, 2-methoxy-6-methyl-	43	4.660	1.20
3	Benzoic acid, methyl ester	58	4.775	1.01
4	Benzeneacetaldehyde, .alpha- l-	94	5.461	2.08
5	Cyclopropane, trimethylmethylene-	25	9.106	2.65
6	cis-1,4-Cyclohexanediol, O,O'-bis (trifluoroacetyl)	59	9.467	2.16
7	3-Methylmannoside	38	12.145	1.24
8	2,2-Diethoxytetrahydrofuran	47	12.259	3.13
9	6-Methyl-2,4-dioxo-1,2,3,4-tetrahy dro-pyrimidine 5-sulfonic acid [2-(2-methyl-1H-indol-3-yl)-ethyl]-amide	59	12.717	3.00
10	Dibutyl phthalate	90	13.718	1.28
11	n-Hexadecanoic acid	99	13.810	5.15
12	9-Octadecenoic acid (Z)-, methyl ester	99	14.857	2.71
13	9-Octadecenoic acid, (E)-	99	15.252	21.21
14	Octadecanoic acid	99	15.383	1.83
15	Methanamine, 1-(4-acridinyl)-	43	16.757	1.62
16	Hexadecane, 1-chloro-	40	18.988	1.61
17	Bis(2-ethylhexyl) phthalate	91	19.498	1.43
18	Sebacic acid, di (3-oxobut-2-yl) ester	43	21.243	1.70

3.3 FTIR Characterization of HUCE and isolated phytomolcules

The FTIR characterization of the crude and that of isolated organic compounds were carried out to identify the functional groups present in them. The FTIR spectra of the extract test solution before immersion, after immersion and that of the washed film on the mild steel were depicted in

Figure. 2(a – c). The IR spectral revealed that the inhibition was as a result of adsorption of –OH stretching, N–H bending, C–O stretching, as well as –C, C–H: C–H bending and C=C stretching functional groups on the mild steel. Similar observation had been observed and reported [12]. The IR spectra peaks in the isolated fractions of HUCE are shown in Figure 3. Table 4 shows IR spectral with their assigned functional group. The strong band of hydroxyl (O-H) groups appeared in all the isolated fractions at peaks (3351- 3310 cm^{-1}), C-H stretch is seen at the peak 2851$cm^{-1}$for alkaloid, saponin and tannin, while at peak 2848cm^{-1} for flavonoid. The C=O stretch is seen at peaks ranging from (1716 -1638 cm^{-1}) for all the isolates. The C-O stretch for the ester functional group occurred at band (1246 – 1014 cm^{-1}) and C-H bending at (921-720 cm^{-1}) for all the isolated fractions. The C-N and N-H stretches appeared at wave numbers of 1336cm^{-1} and 3042 $cm^{-1,}$ respectively, for the alkaloid fraction of *Hunteria umbellata* seed extract [13].

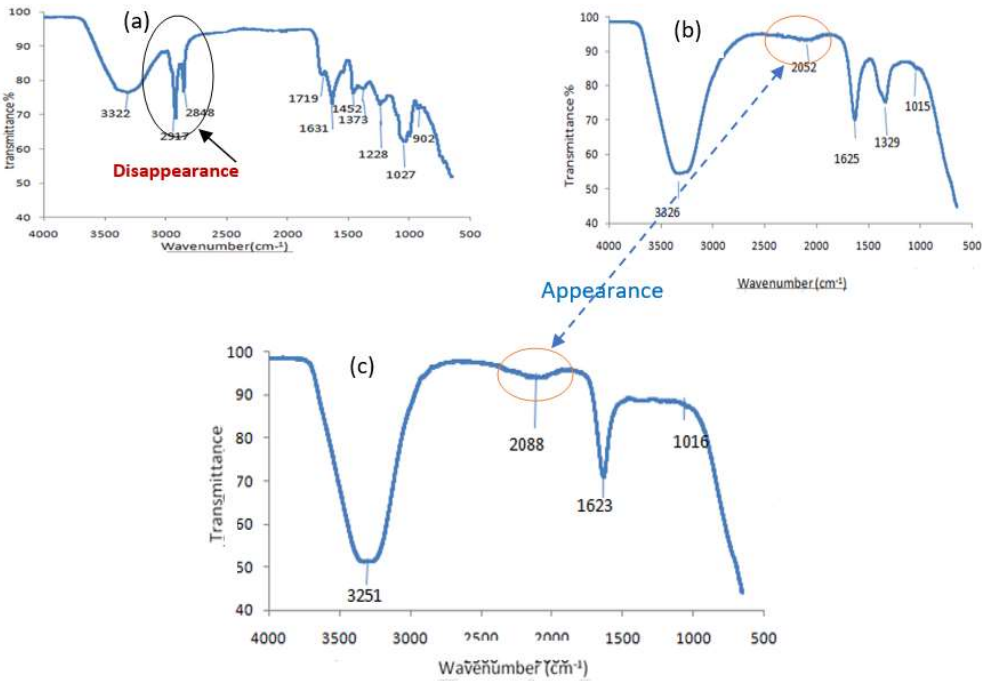


Figure 2: FT-IR spectra for (a) HUCE extract before immersion test (b) extract solution in 1M HCl after test, and (c) washed film adsorbed on mild steel surface

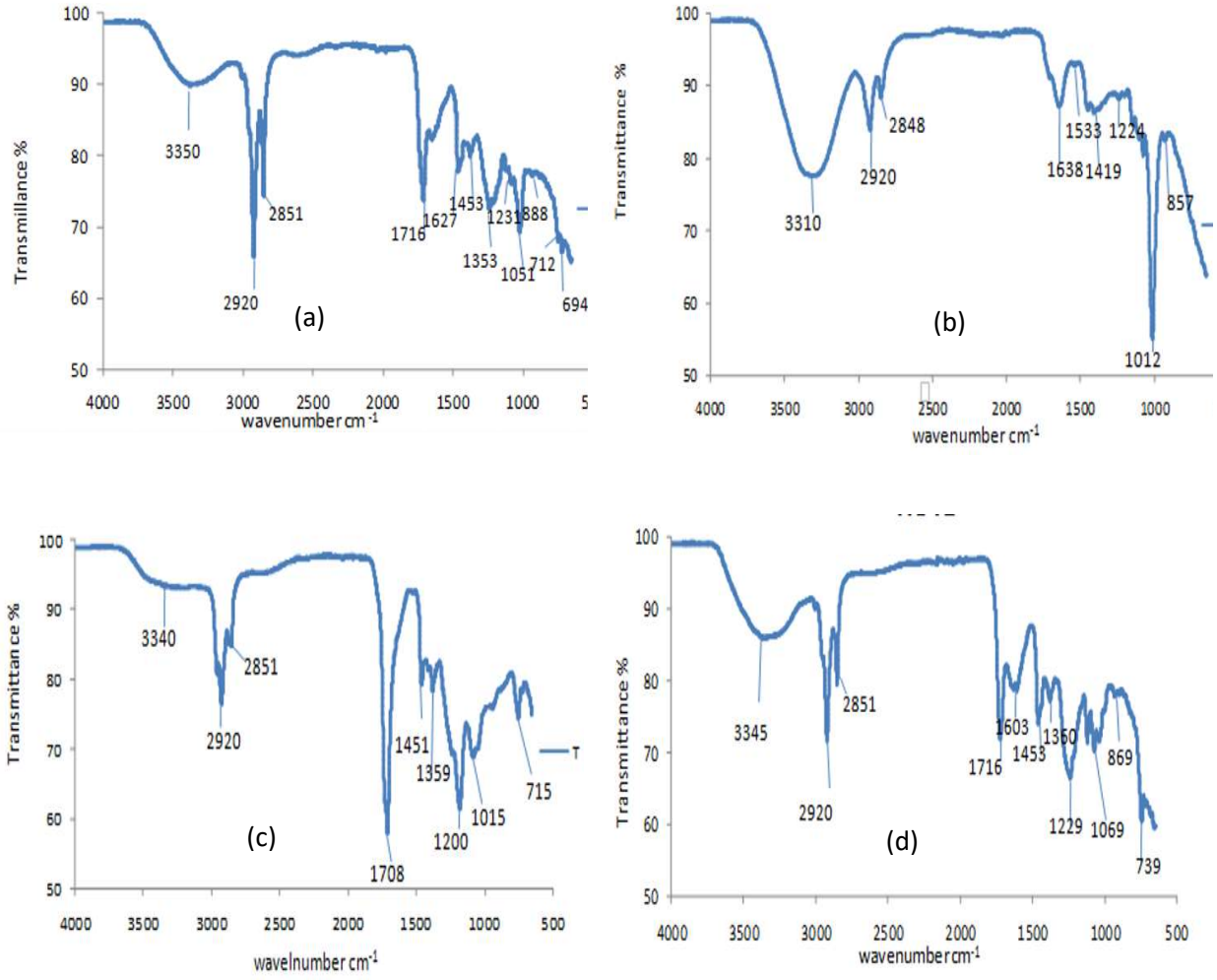


Figure 3 FTIR spectra of the (a) HUAE, (b) HUFE, (c) HUSE and (d) HUTE

Table 4: IR Spectra for the characterisation of isolated phytomolecules of *Hunteria umbellata*

HUCE		HUAE		HUFE		HUSE		HUTE	
IR cm^{-1}	Functional Group	IR cm^{-1}	Functional group	IR cm^{-1}	Functional, group	IR cm^{-1}	Functional, group	IR cm^{-1}	Functional, group
3273	O-H stretch	3350	O-H stretch	3345	O-H stretch	3310	O-H stretch	3340	O-H stretch
2917	C-H stretch	3000, 2920	N-H stretch	2920	C-H stretch	2920	C-H stretch	2920	C-H stretch

2848	C-H stretch	2851, 2591	C-H stretch	2851	C-H stretch	2848	C-H stretch	2851	C-H stretch
1719	C=O, N-H stretch	1707	C=O stretch	1716	C=O stretch	1638	C=O stretch	1708	C=O stretch
1631	C=C alkene stretch	1627	C=C stretch	1603	C=C stretch	1227	C-O-C stretch	1451	C-H group bond
1452	N-O asymmetric stretch	1453	C-H group bonds	1453	C-H groups bonds	1128	C-O stretch	1359	C-O stretch
1373	C-H methyl bending	1353	Aromatic C-N stretching	1360	C-O stretching	1012	C-O stretch	1200	C-O-C stretch
1228	C-N stretch	1231	C-N stretch	1229	C-O stretch	887	C-H out-of-plane bending (aromatic	1015	C-O stretch
1027	C-O stretch	1051	C-O stretch	1069	C-O stretch			715	C-H out-of-plane bending
902	C-H out-of-plane bending	888	C-H out-of-plane bending (aromatic)	869	C-H out-of-plane bending (aromatic				
		712	C-H out-of-plane bending	739	C-H out-of-plane bending (aromatic				
		694	C-H out of plane bending						

3.4 Scanning electron microscopy Analysis

The micrograph of the corrosion inhibited metal immersed in acid, salt and alkaline media, and that dipped barely in these media uninhibited are presented in Figures 4. Figure 4(a, b, c) shows a severely damaged mild steel surfaces immersed in 1M HCl, 1M NaCl and 1M NaOH, respectively**.**SEM micrograph revealed numerous micro pits and cracks as a result of severe attack by the acid, salt and basic solutions. The inhibited system using 1 g/L HUCE (Figure 4d - 4f) however showed protective films on the

surfaces of the metals indicating reduction in corrosion activity in different solutions. The formation of passive layer by adsorbing on the mild steel surfaces of plant extracts have earlier been suggested [14] [15] [16][17][18].

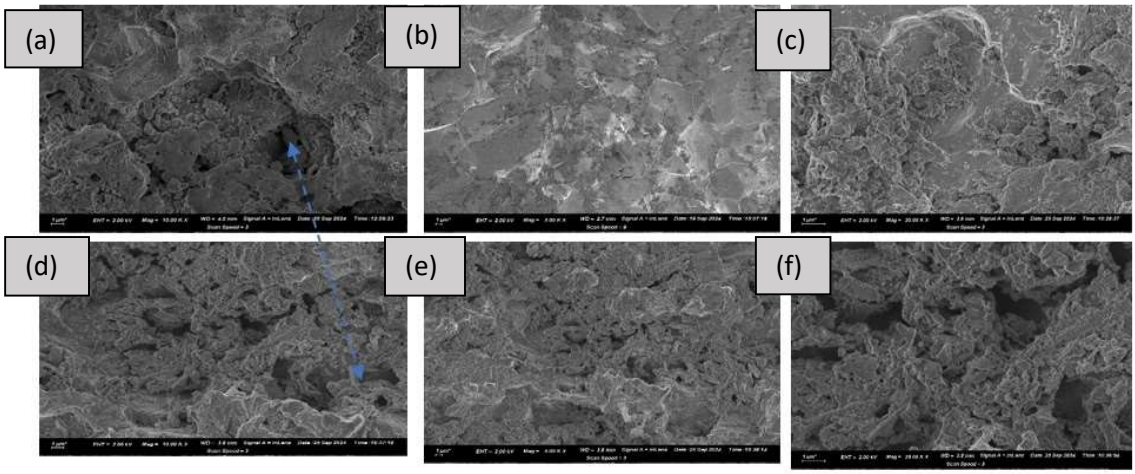


Figure 4 SEM micrograph of mild steel in uninhibited (a) acid solution (b) salt solution and (c) alkali solution compared to respective inhibited system with 1 g/L of *Hunteria umbellata* seed extract (d - f)

3.5 Effect of time and concentration

The effect of time and concentration on the inhibition efficiency of HUCE in different corrosion media at room temperature are shown in Figure 5 (a - c). The inhibition of the metal coupons decreasing with immersion time increases in all media indicating that the inhibitor did not prevent the metals from corroding, it only reduced the rate of corrosion. For HUCE concentration between 0 – 1 g/L, the IE increased from 68.49 to 81.19%, 73.35 to 75.24 %, and 52.86 to 60.90 % for in acid, salt and basic medium, respectively. Increasing the concentration to 1.2 g/L, the IE of 95.17, 85.80 and 82.42% was recorded in the acid, salt and basic solutions, respectively. The recorded value of IE% was due to an increase in the adsorption of inhibitor molecules on the metal surface with time, which form a protective film layer that is responsible for slowing down the rate of corrosion and increasing the efficiency of the inhibition. This observation agreed with earlier reports of [10] and [19].

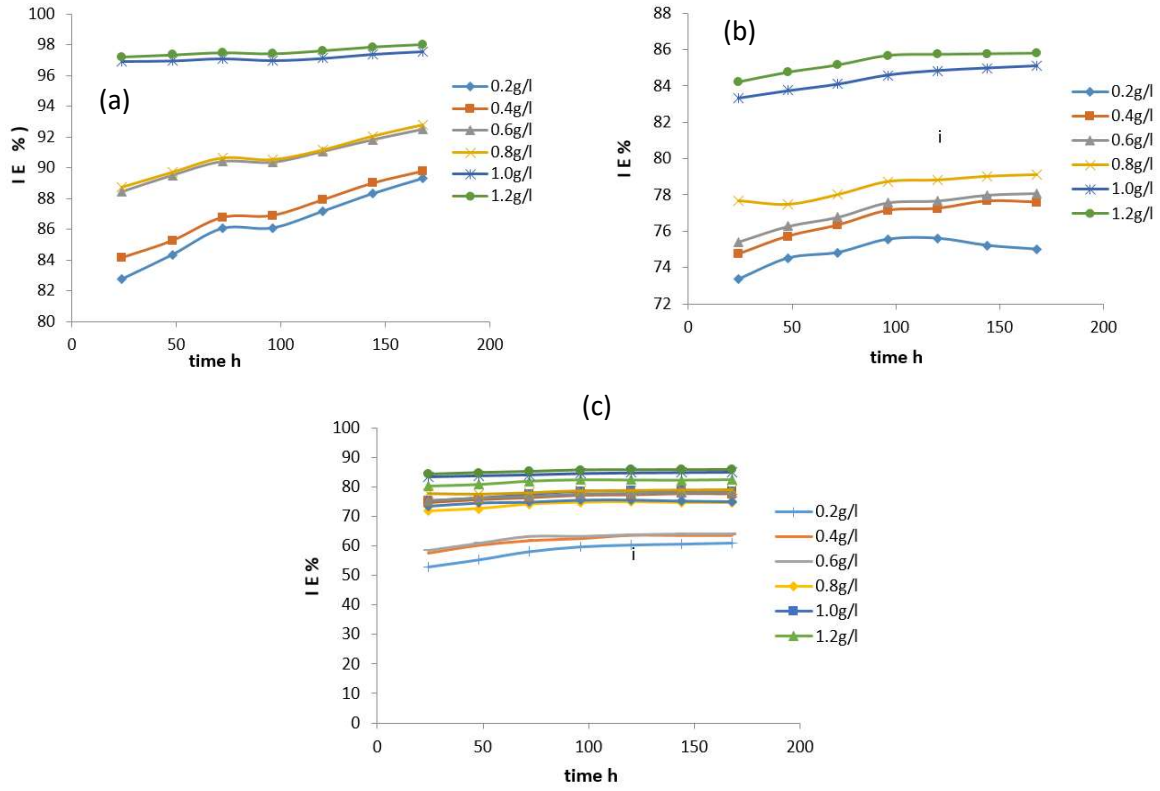


Figure 5: Inhibition efficiency versus immersion time in (a) HCl (b) NaCl and (c) NaOH environment in the presence of different concentrations of HUCE extract

Table 5 presents the IE of alkaloid, saponin, tannins and flavonoid obtained from HUE after they were applied separately on mild steel coupons for 12 h in the acid, salt and alkali medium at different concentrations. In the acid environment, the highest IE of (89.8 %, 86.7 %, 80 % and 77.6%), (83.9%, 81.03 %, 78.3 % and 74.36 %) and (79.60%, 74%, 76.00% and 67.00%) correspond to alkaloid saponin, tannin and flavonoid, in the acidic, salt and alkali media, respectively. These values were however lower compared to their crude extract counterpart. This is attributed to the synergistic effects of the constituent organic compounds in the extract. However, it is observed that the alkaloid exhibited the highest potency than other compounds isolated from HUCE.

Table 5 Corrosion rate and IE of isolated constituents of HUCE on mild steel

		HUAE		HUSE		HUTE		HUFE	
	C0nc (g/L)	CR(g/m2 h)	IE %	CR (g/m^2 h)	IE %	CR (g/m^2 h)	IE %	CR (g/m^2 h)	IE %
	Blank	1.583	-	1.583	-	1.583	-	1.583	-
	0.200	0.490	69.211	0.722	54.386	0.818	48.333	0.840	46.930

1M HCl	0.400	0.440	72.280	0.610	61.491	0.567	64.21	0.592	62.632
	0.600	0.294	81.404	0.403	74.561	0.493	68.860	0.546	65.526
	0.800	0.201	87.280	0.25	84.211	0.411	74.035	0.439	72.281
	1.000	0.161	89.825	0.210	86.754	0.317	80	0.354	77.632
	Blank	0.008	-	0.008	-	0.008	-	0.008	-
1MNaCl	0.200	0.004	52.225	0.004	45.021	0.005	37.606	0.005	35.911
	0.400	0.003	65.466	0.003	63.771	0.003	56.674	0.004	54.873
	0.600	0.003	67.691	0.002	69.280	0.003	63.453	0.003	58.581
	0.800	0.002	78.496	0.002	78.390	0.002	68.538	0.003	66.843
	1.000	0.001	83.898	0.001	81.038	0.002	78.390	0.002	74.364
	Blank	0.005	-	0.005	-	0.005	-	0.005	-
1MNaOH	0.200	0.003	35.740	0.004	22.924	0.003	28.700	0.004	19.675
	0.400	0.003	42.960	0.003	37.726	0.003	43.682	0.003	28.339
	0.600	0.002	61.552	0.002	47.834	0.002	53.249	0.003	42.058
	0.800	0.001	72.563	0.002	67.329	0.001	63.538	0.002	52.346
	1.000	0.001	79.603	0.001	74.007	0.001	76.354	0.002	67.509

3.6 Effect of temperature on IE

Table 6 shows the effects of temperature on corrosion rate and inhibition efficiency of different concentration of HUCE. It was observed that the Corrosion Rate (CR) increases while the Inhibition Efficiency (IE) decreases as the temperature of the system increases, but CR decreases while IE increases as the concentration of the extracts increases. The uninhibited mild steel has a higher corrosion rate compared to the inhibited system as the temperature increases, indicating that various concentrations of the plant extracts inhibit corrosion of mild steel in all the environments studied.

In acid medium at 30^{O}C, the IE of 81.29, 85.18 and 90.14 % were achieved at 0.4, 0.7 and 1.0 g/L, respectively. This shows that the efficiency increases with an increase in concentration. At 60 ^{O}C, the maximum IE of 87.1% was recorded at 1.0 g/L. The reduction of IE as temperature increases was also observed in the salt and basic corrosion media. Similar result was obtained for the measured corrosion depth of attack using a surface roughness tester (Table 7). Thus, mild steel corrosion occurs more rapidly at higher temperatures and therefore the HUCE efficacy reduces as temperature increases. This can be attributed to tendency of the reacting molecules at the elevated temperature to collide faster, leading to more consumption and formation of corrosion products [12] [9]. Furthermore, as the temperature increases, the solution becomes more agitated and the metal dissociates quickly, which results in partial desorption of the adsorbed films from the metal surfaces, leading to high corrosion

rate and low inhibition efficiency [20] [19] and
[12]

Table 6: Effects of temperature and concentrations on the IE of HUCE using weight loss

		1M HCl		1MNaCl		IM NaOH	
T (K)	**Conc. (g/L)**	**CR $g/m^2 h$**	**IE (%)**	**CR $g/m^2 h$**	**IE (%)**	**CR $g/m^2 h$**	**IE (%)**
303	0.00	16.70	-	10.20	-	7.01	-
	0.40	3.14	81.30	3.60	64.80	2.97	57.70
	0.70	2.49	85.20	2.76	72.90	1.86	73.50
	1.00	1.65	90.10	2.38	76.70	1.43	79.60
318	0.00	30.60	-	41.90	-	29.30	-
	0.40	7.55	75.30	18.90	54.90	12.80	56.50
	0.70	5.44	82.20	14.80	64.70	10.30	64.90
	1.00	3.96	87.10	12.10	71.10	7.85	73.20
333	0.00	57.71	-	65.40	-	51.35	-
	0.40	14.90	74.10	30.30	51.60	23.72	53.80
	0.70	10.82	81.20	22.90	63.30	19.47	62.07
	1.00	8.29	85.60	18.60	70.20	14. 35	72.06

Table 7: Surface depth parameter (Rz) at different temperature and concentration of HUCE for mild steel in corrosive environment after immersion time of 12h

		1 M HCl			1 M NaCl			1 M NaOH		
T (K)	Conc. (g/L)	R_Z (µm)	IE (%)	Ɵ	R_Z (µm)	IE (%)	Ɵ	R_Z (µm)	IE (%)	Ɵ
303	0.00	2.76	-		1.53	-	-	1.29	-	-
	0.40	0.52	81.30	0.81	0.54	64.80	0.65	0.55	57.7	0.58
	0.70	0.41	85.20	0.85	0.41	72.90	0.73	0.34	73.5	0.74
	1.00	0.27	90.10	0.90	0.36	76.70	0.77	0.26	79.6	0.80
318	0.00	9.25	-	-	8.42	-	-	7.02	-	-
	0.40	2.28	75.10	0.75	3.80	54.9	0.55	3.05	56.51	0.57
	0.70	1.64	82.20	0.82	2.97	64.7	0.65	2.46	64.9	0.65
	1.00	1.19	87.10	0.87	2.43	71.1	0.71	1.88	73.2	0.73
333	0.00	17.02	-	-	15.51	-	-	13.62	-	-
	0.40	4.41	74.10	0.74	7.51	51.6	0.52	6.29	53.80	0.54
	0.70	3.20	81.20	0.81	5.69	63.3	0.63	5.17	62.07	0.62
	1.00	2.45	85.60	0.86	4.62	70.2	0.70	3.81	72.06	0.72

3.7 Isotherm, kinetics and thermodynamic studies

Table 8 shows the isotherm parameters obtained at different corrosion media after 12 h immersion time. The three isotherms described the mechanism of inhibition; however, the best isotherm is the Langmuir isotherm with highest and consistent correlation factors (R^2> 0.999). Thus, the inhibitor under study obeys the Langmuir adsorption isotherm which assumed no interaction between adsorbed molecules on the surface [18][7]. Similarly, judging by the value of correlation coefficient (R- square), it is evident from Table 9that the corrosion inhibition followed pseudo-second-order (R^2: 0.999–1) for concentration (0.4 -1 g/L), temperatures (303–333 K) and time (0–12 h) in all the media investigated.

Table 10 shows the average thermodynamic parameters estimated across the three media in the absence and presence of different

concentrations of HUCE at different temperatures. The activation energy of the system increases with the inhibitor concentration and temperature. It ranges between 34.5 and 47.3 kJ/mol which is less than 80KJ/molindicating physical nature of the adsorption process [18]. The positive average enthalpy change indicates an endothermic process. Large and negative values of entropies implya decrease in disorderliness [21][9] and [1].

Table 8: Isotherm parameters of *Hunteria umbellata* seed extract for corrosion inhibition of mild steel in 1M HCl, 1M NaCl and 1M NaOH after 12 h immersion time at different temperatures

		1M HCL			1MNaCL			1MNaOH		
		303K	**318K**	**333K**	**303K**	**318K**	**333K**	**303K**	**318K**	**333K**
	Slope	1.028	1.029	1.047	1.142	1.180	1.081	1.023	1.068	1.118
	Inter	0.087	0.123	0.123	0.160	0.280/	0.339	0.231	0.221	0.277
Langmuir	**K_{ads}**	11.490	8.130	8.130	6.250	3.570	2.950	4.330	4.520	3.610
	- ΔG	16,269.	16,159.	16,921	10,387	10,784	11,264	13,810	14,610	14,674
	R^2	0.998	0.999	0.999	1.000	0.999	0.999	0.999	0.997	0.999
	Slope	0.11	0.157	0.158	0.187	0.282	0.341	0.266	0.271	0.273
	Intercept	-0.047	-0.060	-0.066	-0.112	-0.147	-0.148	-0.096	-0.109	-0.142
	N	9.090	6.369	6.329	5.348	3.546	2.933	3.759	3.690	3.663
Freundlich	**K**	0.897	0.871	0.859	0.773	0.713	0.711	0.802	0.778	0.721
	- ΔG	9,845	10,253	10,698	9,469	9,724	10,177	9,562	9,956	10,214
	R^2	0.967	0.999	0.999	0.991	0.999	0.987	0.997	0.953	0.999
	Slope	0.217	0.294	0.284	0.303	0.405	0.472	0.562	0.489	0.459
	Intercept	0.895	0.809	0.856	0.870	0.710	0.707	0.805	0.78	0.72
Temkin	**A**	-5.307	-3.917	-3.984	-3.800	-2.843	-2.439	-2.049	-2.355	-2.509
	K	13,317	903.25	916.04	743.51	56.635	31.468	27.063	39.363	37.036
	- ΔG	34,042	28,613	30,001	26,774	21,292.	20,669.	18,427	20,330	21,120
	R^2	0.961	0.998	0.999	0.993	0.989	0.994	0.985	0.953	1.000

Table 9: Kinetic parameters for the pseudo-first order and (b) pseudo-second order at 1.0g/L concentration and different temperatures

Pseudo First Order									
		IM HCl			**1MNaCl**			**1MNaOH**	
Temp	**303K**	**318K**	**333K**	**303K**	**318K**	**333K**	**303K**	**318K**	**333K**
Slope	-0.346	-0.466	-0.289	-0.308	-0.36	-0.236	-0.252	-0.291	-0.321
Intercept	-2.872	-1.92	-2.708	-2.357	-2.362	-2.045	-2.079	-2.366	-1.356
k/hr	0.346	0.466	0.289	0.308	0.36	0.236	0.252	0.291	0.321
Θvalue	0.0566	0.1466	0.067	0.0947	0.0942	0.129	0.125	0.0939	0.258
Θexp	0.900	0.870	0.850	0.800	0.730	0.715	0.760	0.710	0.700
R²	0.89	0.951	0.710	0.509	0.782	0.910	0.887	0.501	0.864
Pseudo-Second Order									
Slope	1.106	1.142	1.163	1.220	1.340	1.350	1.276	1.379	1.425
Intercept	0.059	0.101	0.124	0.409	0.420	0.655	0.484	0.475	1.081
k/hr	20.731	12.914	10.909	3.639	4.275	2.783	3.365	4.004	1.889
Θvalue	0.904	0.876	0.860	0.829	0.746	0.741	0.784	0.725	0.702
Θexp	0.900	0.870	0.850	0.800	0.730	0.715	0.760	0.710	0.700
R²	0.999	0.999	0.999	0.999	0.999	0.999	0.999	0.999	0.999

Table 10: Average thermodynamic parameters

Temperature (K)	**Conc (g/L)**	**ΔH (KJ/mol)**	**Δ5 (J/mol K)**	**ΔE_A (KJ/mol)**	**A**
		4hr			
303	0	32.890	-186	35.540	5.7×10^{7}
	0.400	41.312	-90.450	43.950	3.38×10^{8}
	0.700	38.860	-100.600	41.500	9.99×10^{7}
	1.000	44.621	-178.020	47.260	6.35×10^{8}
		8hr			
	0	32.017	- 187.410	34.661	2.16×10^{7}
318	0.400	40.755	- 185.000	43.390	1.4×10^{8}
	0.700	38.468	-186.000	41.104	4.4×10^{7}
	1.000	43.366	- 187.160	46.001	2.05×10^{8}
		12hr			
	0	31.859	-187	34.503	1.4×10^{7}
333	0.400	41.021	-185.800	43.656	1.07×10^{8}
	0.700	41.129	-180.298	41.129	3.09×10^{7}
	1.000	42.484	-185.870	45.120	9.99×10^{9}

3.8 Application of HUCE in alkyd paint

Figure 6 shows the percentage of weight loss for all the coated samples with or without inhibitor immersed in corrosive environment for five weeks. During the first week, the coated mild steel without inhibitor experienced the highest

weight loss of 5.3 – 5.7%. The weight loss however reduces to about 4.1, 3.9, and 3.77 % on the introduction of 0.30, 0.45 and 0.60 wt.% inhibitor into the paint. The weight loss increases with the immersion period, and remains fairly constant after the third weeks. The trend observed in coated samples without HUCE extract loading is also seen in the incorporation of plant extracts.

However, the weight-loss percentage difference between extracts at 0 % and those at 0.3, 0.45, and 0.6 % decreases as the immersion time increases. This is because of the corrosion activity brought on by moisture seeping through the capillaries or voids in the coating [22]. When moisture enters the pores and is attracted to any polar functional groups in the coating, water permeation takes place. Water penetration into the alkyd coating is restricted by the dissociation of the OH functional groups brought on by the addition of HUCE extracts [23].

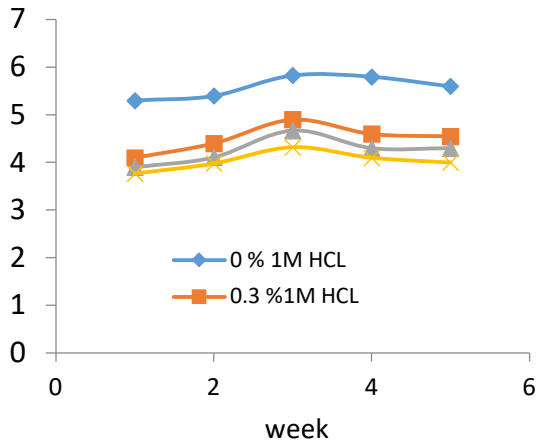


Figure 6 Graph showing percentage weight loss against the immersion period (weeks) for HUCE - Alkyd coating

4.0 Conclusion

1.The extracts of *Hunteria umbella* seed with their isolated phytomolecules showed good inhibition characteristics for mild steel in corrosive media due to the presence of alkaloid, tannins, saponins, and O-H, C-N, C=O and unsaturated functional groups which were identified by the GC - MS and FTIR analyses.

2. The inhibition efficiency increased with increase in concentration but decreased with increase in temperature in all the corrosive media. The results produced by the two methods of corrosion analysis (weight loss and depth profile measurement) were in a very good agreement with one another. The performance of all the tested inhibitors in the three corrosive media followed the order 1M HCl > 1M NaCl > IM NaOH.

3. The adsorption of extract film was found to follow Langmuir isotherm and pseudo-second-order kinetics. The values of thermodynamic parameters obtained suggested that theadsorption mechanism of HUCE on the mild steel is physiosorption, spontaneous and endothermic in nature.

4. With very low weight loss obtained by the addition of the extracts of the HUCE to the alkyd coating applied on the mild steel, it is evident that the extract can be use as anti-corrosive additive in coating.

References

1. Nya N.E, Ikeuba A.I, Okafor P.C, Ugi B.U, Bassey V.M, and Obike A.I, (2018). Mild SteelCorrosion Mitigation in Sulphuric Acid via Benign Isolated Phytochemical from *viscumalbium. Journal of Material science and Chemical Engineering* 6, 132- 146.
2. Ogunleye, O.O., Eletta, O.A., Arinkoola, A.O and Agbede, O.O., (2018). Gravimetric and quantitative surface morphological studies of Mangifera indica peel extract as a corrosion inhibitor for mild steel in 1 M HCl solution. *Asia Pac. J. Chem. Eng*., e2257
3. Faiz .M, Zahari. A, Awang. K, and Hussin .H. (2020). Corrosion Inhibition on Mild Steel in 1M HCl Solution by *Cryptocaryanigra* extracts and three of its Constituents (Alkaloids). *Royal Society of Chemistry.10*, 6547- 6562.
4. Ricky, E. X., Lugwisha, E. H. J., and Philip, J. Y. N. (2021). Corrosion Inhibition of Mild Steel in Seawater by 2 , 4 , 6-Triamino-3-Pentadecylphenyl Acetate Derived from Cashew Nut Shell. *Liquid*. *47*(1): 112–122.
5. Ogunleye. O.O., Arinkoola . A.O., Eleta . O.A., Agbede O. O.,Osho .Y. A., Morakinyo . A.F and Hamed.J. O. (2020). Green Corrosion Inhibition and Adsorption Characteristics of *Luffa Cylindrica* leaf extract on Mild Steel in Hydrochloric Acid Environment. *Heliyon* 6, 1-12.
6. Chapagain. A, Acharya. D.Das. A. K., Chnetri K., Oli B. H and Yadav A.P. (2022). Alkaloid ofRhynchosstylisretusa as GreenInhibitors for Mild Steel Corrosion in 1M H_2SO_4 Solution. *Electrochemistry.3*, 211-224.
7. Arinkoola, A. O., Oyelade, E. F., Omowumi, M., Akinyemi, A. G., & Alagbe, S. O. (2024). Quantifying Uncertainty of Green Inhibition Efficiency of Luffa Cylindrica Leaf Extract on Mild Steel in Acidic Medium. *Journal of Chemical and Petroleum Engineering (JChPE)*,
8. Ikemba A. I., and Okafor P. C., (2018) "Green corrosion protection for mild steel in acidic media: saponins and crude extracts of Gongronemalatifolium", *Pigment and Resin Technology*, https://doi.org/10.1108/PRT-03-2018-0020
9. Ugi, B.U., Bassey,V.M., Obeten, M.E., Adalikwu, S.A. and Nandi,D.O. (2020) Secondary Plant Metabolitesof Natural Product Origin—Strongylodonmacrobotrys as Pitting Corrosion Inhibitorsof Steel around Heavy Salt Deposits inGabu, Nigeria. Journal of Materials Scienceand Chemical Engineering, 8, 38-60.https://doi.org/10.4236/msce.2020.85004
10. Ogunleye.O.O., Arinkoola .A.O., Alagbe, S.O., Agbede .O.O., Omodele .A.E., Morakinyo .A. F. and Osho . Y.A. (2019). Synthesis of Green Inhibitor for Mild Steel in Acidic Environment. *Indian Chemical Engineer*. 0(0), 1-15
11. Zakeri. A, Bahmani. E, Sabour A.A, and Aghdam. R, (2022). Plant Extracts as a Sustainable and Green Corrosion Inhibitors for Protection of Ferrous Metals in Corrosive Media: A Mini Review. *Corrosion Communications* 5, 25-38.
12. Alaneme. K. K., Olusegun. S. J., and Adelowo .O.T., (2015). Corrosion Inhibition and Adsorption Mechanism Studies of *Hunteria umbellate* Seed Husk Extracts on Mild Steel Immersed in Acid Solution. *Alenxandria Engineering Journal*, *1*,1-10
13. Chapagain, A., Acharya, D., Das, A. K., Chhetri, K., Oli, H. B., Yadav, A. P., & Asia, S. (2022). *Alkaloid of Rhynchostylis retusa as Green Inhibitor for Mild Steel Corrosion in 1 M H 2 SO 4 Solution can*. 211–224.
14. Emembolu, L. N. Achugbu O. E., and Onukwuli O. D. (*2022,*)Bioinhibition of Corrosion of Mild Steel in 1 M NaOH by Ethanolic Extract of *Dialiumguineense*Leaves Using Different Corrosion Techniques*Manila Journal of Science* 15(2)pp. 1–18
15. Faiz, M., Zahari, A., Awang, K., & Hussin, H. (2020). Corrosion inhibition on mild steel in 1 M HCl solution by: Cryptocarya nigra extracts and three of its constituents (alkaloids). *RSC Advances*, *10*(11), 6547–6562. https://doi.org/10.1039/c9ra05654h
16. Diaz M Y, Valladares M G, Menchaca E C and Uruchurtu J (2020). Electrochemical Evaluation of Chrysin Flavonoid as Corrosion Inhibitor for Mild Steel in

Sulphuric Acid Solution.*European Journal of Engineering Research and Science* Vol. 5, No. 11 DOI: http://dx.doi.org/10.24018/ejers.2020.5.11.2247

17. Ramakrishnan P. J, Janardhanan V. D. K,Sreekumar R , and Mohan K. P.,(2014) Investigation on the Effect of Green Inhibitors for CorrosionProtection of Mild Steel in 1M NaOH SolutionHindawi Publishing CorporationInternational Journal of CorrosionVolume 2014, Article ID 487103, 5 pageshttp://dx.doi.org/10.1155/2014/487103

18. Nnanna L, Nnanna G, Nnakaife J, Ekekwe, N, Eti P (2016) Aqueous Extracts of *Pentaclethra macrophylla Bentham* Roots as Eco-Friendly Corrosion Inhibition for Mild Steel in 0.5 M KOH Medium International Journal of Materials and Chemistry. 6(1):12-18 DOI: 10.5923/j.ijmc.20160601.03

19. Al-Dokheily M. E, Kredy H. M., Al-Jabery R N., (2014) Inhibition of Copper Corrosion in H2SO4, NaCl and NaOH Solutions by *Citrullus colocynthis*Fruits Extract Journal of Natural Sciences Research www.iiste.org ISSN 2224-3186 (Paper) ISSN 2225-0921 (Online) Vol.4, No.17,

20. Kasim A. (2013). Plant Extract Nano particles Hybrid as Corrosion Inhibition for AA2024 Aluminium Alloy. Ph.D. Dissertation. Ahmadu Bello University, Zaria.pp 1-304.

21. Abeng F. E. and Idim V.D. (2018). Green Corrosion Inhibitor for Mild Steel in 2M HCl solution Flavonoid extract of *Eriugeronflorabumdus*; *World scientific News International science Journal.98*, 89-98

22. Sung, S. J., Kim, T., Park, J., So, S. H., Choi, J., Yang, S. J., & Park, C. R. (2017). Influence of the physicochemical characteristics of reduced graphene oxides on the gas permeability of the barrier films for organic electronics. *Chemical Communications*, *53*(49), 6573-657

23. ZulkifliM.F. R, Bahrin. S.S, Abdullahi.S., Ghazali.M. S. M, and Wanik.W. M. N. (2021) *Citrus Aurantifolia* leaf Extract as a Potential Anti-Corrosion Additives in Alkyd Paint for Mild Steel. *Journal of Sustainable Science and Management*. 3, 10-20. http://doi.org/10.46754/jssm.2021.04.00.